Deformation of Polyelectrolyte Brushes in Strong Flows: Good Solvent Regime

J. L. Harden,*,†,‡ O. V. Borisov,§ and M. E. Cates‡

Cavendish Laboratory, Cambridge University, Madingley Road, Cambridge CB3 0HE, U.K., Department of Physics and Astronomy, University of Edinburgh, James Clerk Maxwell Building, King's Buildings, Mayfield Road, Edinburgh EH9 3JZ, U.K., and Max-Planck-Institut für Polymerforschung, Postfach 3148, D-55021 Mainz, Germany

Received August 14, 1996; Revised Manuscript Received November 14, 1996[⊗]

ABSTRACT: We study theoretically the deformation of polyelectrolyte brushes in strong flows of good solvent using a scaling theory which calculates the deformation of grafted chains and the solvent flow profile within the brush in a mutually consistent fashion. We consider the cases of permeation flows normal to the grafting surface and shear flows parallel to the grafting surface. For the case of permeation flows, we find that strongly charged brushes are more uniformly extended than weakly charged ones and that the crossover region separating the weak deformation and strong deformation regimes shifts to higher solvent flow rates and becomes somewhat broader with increasing charge fraction. For the case of shear flows, we find that chains are more uniformly stretched and less strongly tilted with increasing charge fraction. Furthermore, we demonstrate that with increasing charge fraction, there is a reversal of the dependence of brush thickness on shear rate: weakly charged brushes expand in strong shear flows, while strongly charged brushes collapse somewhat in the same flows, in qualitative agreement with previous theoretical predictions.

1. Introduction

The properties of polymer brushes (polymers irreversibly attached by one end to a surface at high grafting density) have been the subject of intensive study during the past two decades. The equilibrium properties of neutral polymer brushes are now well established.[1,2] Recently, there has also been substantial progress toward understanding the equilibrium properties and structure of polyelectrolyte brushes (densely grafted layers of charged polymers).[3−12] Due to the solubility of charged polymers in polar solvents, polyelectrolyte brushes are of particular interest for the stabilization of colloids and the modification of interface properties in aqueous environments, for use in drug delivery systems, and for bioengineering applications.

Many recent studies have focused on the steady-state response of grafted layers to applied perturbations, such as the hydrodynamic drag due to solvent flows in the neighborhood of grafted layers and the frictional forces due to the relative motion of brush-bearing surfaces in contact.[13−26] The response of grafted polymer layers to flows has important implications for the rheological behavior of colloidal dispersions stabilized by polymer layers, for the lubrication properties of polymer-coated surfaces, and for the permeability characteristics of brush-bearing porous media, such as selective filtration membranes. Of particular interest is the limit of strong flows, in which there is significant deformation of grafted layers, and, in principle, modification of the flow due to this deformation. Such strong flow conditions can give rise to novel and unexpected brush behavior. For example, in the case of neutral polymer brushes subjected to shear flows of good solvent, there is evidence that the brushes can swell in the direction normal to the grafting surface in response to sufficiently high shear-rate flows parallel to the grafting surface.[13−16]

Early theoretical models of such brush deformation phenomena[19−22] are based on the nonlinear response of tethered chains to large forces applied to the free chain ends.[27] In the case of sheared neutral brushes in good solvent conditions, such approaches can predict swelling behavior that is in qualitative agreement with the experiments of refs 13−16. On the other hand, for the case of polyelectrolyte brushes in good solvent shear flows, such an approach predicts deswelling behavior for sufficiently charged systems.[22] However, quantitative comparison of these theoretical predictions with experimental results is difficult since the solvent shear rate $\dot{\gamma}$ is the relevant experimental control parameter and its relation to the effective boundary shear force utilized in these models is not known *a priori*. Furthermore, since such approaches effectively ignore brush−solvent hydrodynamics, the details of the solvent flow profile inside a brush and the associated internal stucture of a deformed brush cannot be elucidated. Indeed, individual tethered chains subjected to forces applied to the chain ends are uniformly extended,[27] whereas such tethered chains subjected to solvent flows are predicted to deform in a nonuniform fashion.[28]

Recently, a theoretical approach for studying the deformation of grafted layers of neutral polymers in strong flow conditions was introduced which calculates the deformation of grafted chains and the solvent flow profile within the layer in a mutually consistent fashion.[24,25] The predictions of this model for the swelling of neutral brushes in shear flows of good solvent are in qualitative accord with the predictions of ref 20 and in semiquantitative accord with the experimental results of refs 13−16. Furthermore, this approach has provided useful insights into the detailed deformation behavior of densely grafted chains in strong flows and the nature of the coupling between flow and brush deformation.

In this paper we examine the behavior of polyelectrolyte brushes in strong flows of good solvent within the framework of a generalized version of the model of refs 24 and 25. In doing so, we focus on the dependence of polyelectrolyte brush deformation in flow on the

* Present address: Department of Chemical Engineering, Johns Hopkins University.
† Cambridge University.
‡ University of Edinburgh.
§ Max-Planck-Institut-für Polymerforschung.
⊗ Abstract published in *Advance ACS Abstracts,* January 15, 1997.

S0024-9297(96)01233-8 CCC: $14.00

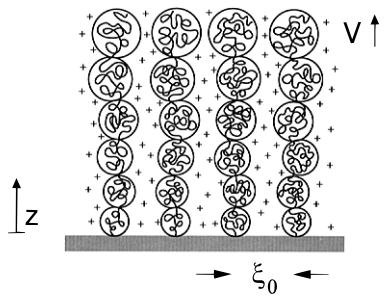

Figure 1. Sketch of an extended polyelectrolyte brush in a solvent permeation flow $\mathbf{V}(z) = +V\hat{z}$ normal to the grafting surface.

fraction of charged groups per chain in the absence of added salt. We consider two types of solvent flows: simple shear flow parallel to a planar grafting surface, and permeation flow perpendicular to the grafting surface. The latter flow type can occur, for instance, when polymers grafted to a porous surface are subject to hydrodynamic pressure gradients normal to the polymer layer. In section 2, we introduce our model and apply it to polyelectrolyte brush deformation in uniform permeation flows of good solvent perpendicular to the grafting surface. In section 3, we extend the model to the case of brush deformation in simple shear flows parallel to the grafting surface. Finally, in section 4, we conclude the paper with a short discussion of our results.

2. Permeation Flows

Consider a brush consisting of monodisperse charged chains of degree of polymerization N and monomer size a in salt-free, good solvent conditions grafted at areal density $\sigma \sim \xi_0^{-2}$ to a flat porous medium. We consider the case of extending flows, in which the brush is subjected to a flow $\mathbf{V} = +V\hat{z}$ perpendicular to the grafting surface, as sketched in Figure 1. We assume that a fraction α of the monomers are charged, say negatively, and that the chains are sufficiently charged that the αN positive counterions per chain are essentially confined within the brush, implying its electroneutrality as a whole (*i.e.* the electrostatic screening length due to counterions is smaller than the brush thickness). As has been discussed in ref 9, this total electroneutrality of the brush implies its local electroneutrality as well, provided that the polyelectrolyte density profile is slowly varying on the scale of the electrostatic screening length. The polyelectrolyte effects in the brush are expected to be strong in the range of parameters (α,σ) corresponding to the local electroneutrality conditions[9] under which the Debye length λ_D obeys $\xi_0 \ll \lambda_D \ll H$, where H is the brush thickness. We mainly restrict our consideration to this case, but in section 2.4 we briefly address the "capacitor regime" of $\lambda_D \gg H$.

For simplicity, our analysis adopts the Alexander–de Gennes ansatz that all chains behave alike.[29,30] Thus, we represent the chains in the perturbed brush as strings of excluded-volume blobs and assume that all chain ends are at the outer edge of the brush. We remark that this approach is more reasonable for brushes subjected to external stretching forces than for undeformed brushes, in which strong fluctuations of the positions of free chain ends occur.[31,32]

For very weakly charged (or sufficiently densely grafted) brushes in the absence of flow, this scaling approach results in a brush of thickness $H_0 = N\xi_0^{-2/3}\nu^{1/3}a^{5/3}$ formed of close-packed blobs of size ξ_0, where $\nu \sim (T - \Theta)/T$ is a dimensionless second virial coefficient which scales with reduced temperature difference from the Θ point. Thus, polyelectrolyte brushes in this limit behave as neutral ones. On the other hand, for more strongly charged quiescent brushes, this scaling approach results in a brush of thickness $H_e = N\alpha^{2/5}\nu^{1/5}a$ formed of extended strings of blobs of size $\xi_e = \alpha^{-3/5}\nu^{1/5}a$.[9] As a rough rule of thumb, one may think of such a strongly charged equilibrium brush as a string of good solvent blobs that contain one charge per blob.[5] The crossover between "quasi-neutral" and polyelectrolyte behavior of the brush corresponds to the condition $\xi_0 \cong \xi_e$ (see ref 9 for detailed discussion). In all cases, we will restrict our attention to good solvent conditions for which $\nu > \nu_* \simeq a/\xi_0$.

In the presence of flow, we represent the chains in the perturbed brush as strings of Pincus blobs.[27] Since the chain extension is due to the integrated hydrodynamic drag on each chain rather than a force applied to the chain ends, the blob size ξ is not constant, but is a function $\xi(z)$ of the distance z from the grafting plane which must be determined.

2.1. Free Energy and Effective Tension. The free energy per chain is the sum of four terms: an elastic term F_{el} involving chain deformation, an osmotic term F_{int} involving excluded volume interactions between blobs, a mixing term F_{ion} accounting for the entropy of mixing of the free counterions, and an electrostatic term F_{ch} accounting for the correlations of charge density. This paper focuses on the limit $\alpha \ll (l_B/a)^{-2}$, where $l_B \cong e^2/\epsilon kT$ is the Bjerrum length characterizing the strength of the Coulomb interactions (e is an elementary charge and ϵ is the dielectric constant of the solvent), in which F_{ch} is negligible compared with F_{ion}.[33] The expressions for F_{el} and F_{int} retain the forms derived in ref 24 for neutral brushes in extending permeation flows. The elastic energy per chain is obtained by considering each chain as an elongated string of blobs and may generally be written as

$$\frac{F_{el}}{k_B T} \simeq \int_0^H \frac{dz}{\xi(z)} \tag{1}$$

where H is the thickness of the deformed brush. The blob size ξ is related to the number of monomers in a blob g via $\xi \sim g^{3/5}\nu^{1/5}a$. The interaction between chains may be approximated by a virial expansion in the blob density.[19,20] The local interaction energy per blob is of order $kT[\xi(z)/\xi_0]^2$ and leads to an interaction energy per chain of the form

$$\frac{F_{int}}{k_B T} \simeq \xi_0^{-2}\int_0^H dz\ \xi(z) \tag{2}$$

where $\xi_0 \sim \sigma^{-1/2}$ is the average separation between grafting points. The ion term F_{ion} is estimated from the entropy of mixing of a gas of counterions which is constrained to follow the local monomer density in the normal $\hat{z}$ direction due to the local electroneutrality ansatz. Consider the counterions associated with a blob $\xi(z)$ at a distance z from the grafting surface. There are of order $\alpha g(z)$ counterions associated with this blob, distributed freely in a volume $V \simeq \xi_0^2\xi(z)$. The counterion mixing entropy *per blob* scales as $k_B T\phi_c V \log \phi_c$, where $\phi_c(z) \sim \alpha g a^3/V$ is the average local counterion volume fraction. Using $g \sim (\xi/a)^{5/3}\nu^{-1/3}$ then leads to a counterion entropy of mixing contribution F_{ion} per chain

of the form

$$\frac{F_{\text{ion}}}{k_{\text{B}}T} \simeq \alpha\nu^{-1/3}a^{-5/3}\int_0^H \mathrm{d}z\ \xi(z)^{2/3}\log\left[\frac{\alpha\xi(z)^{2/3}a^{4/3}}{\nu^{1/3}\xi_0{}^2}\right] \quad (3)$$

The total free energy per extended chain F is given by the sum of eqs 1−3. Note that all numerical prefactors, unknown but assumed to be of order unity, have been suppressed in these expressions. Following the procedure developed in ref 24 for neutral brushes, we use this chain free energy to define an effective local chain tension $t(z)$ as follows. Consider a infinitesimal section of chain of length Δz containing Δn monomers. Equations 1−3 give the free energy of this section of chain as

$$\Delta F \sim kT\left(\frac{1}{\xi(z)} + \frac{\xi(z)}{\xi_0{}^2} + \frac{\alpha\xi(z)^{2/3}}{\nu^{1/3}a^{5/3}}\log\left[\frac{\alpha\xi(z)^{2/3}a^{4/3}}{\nu^{1/3}\xi_0{}^2}\right]\right)\Delta z \quad (4)$$

This expression may be written exclusively in terms of Δz and Δn by using the Pincus law[27] for chain stretching, $\Delta z \simeq (\Delta n/g)\xi = \Delta n\xi^{-2/3}\nu^{1/3}a^{5/3}$, to eliminate ξ from ΔF. Subsequent variation of ΔF with respect to Δz at fixed Δn, and use again of the Pincus law, yields the effective local chain tension

$$t(z) = kT\left(t_1\frac{1}{\xi(z)} - t_2\frac{\xi(z)}{\xi_0{}^2} - t_3\frac{\alpha\xi(z)^{2/3}}{\nu^{1/3}a^{5/3}}\right) \quad (5)$$

where t_1, t_2, and t_3 are positive constants of order unity. This effective tension determines the local departure from equilibrium of a representative chain, under conditions where all chains are constrained to behave identically. It already contains osmotic terms and so should not be confused with the (purely elastic) chain tension in a deformed chain which, within a nonscaling, mean field approach to brushes, is balanced by osmotic pressure gradients. The unknown constants in eq 5 may be fixed by insisting on equilibrium chain behavior in the limit of vanishing effective chain tension. For $\alpha = 0$, we recover the Alexander−de Gennes result, $\xi = \xi_0$, if $t_1 = t_2$. On the other hand, in the large charge fraction limit, we recover the equilibrium polyelectrolyte result, $\xi_{\text{e}} = \alpha^{-3/5}\nu^{1/5}a$, if we set $t_1 = t_3$. So, for definiteness, we set $t_1 = t_2 = t_3 = 1$ here and in the following.

2.2. Hydrodynamic Forces. The local Pincus blob size $\xi(z)$ is obtained by balancing the differential chain tension across a blob with the total effective hydrodynamic drag on the blob. For polyelectrolyte chains, there are in principle two sources of drag. First, there is the direct hydrodynamic drag on each blob, as in the neutral chain case.[24] For Zimm−Stokes blobs, this drag per blob scales as $\eta\xi(z)V$, where η is the solvent viscosity. Second, when the counterions are confined to the brush and when there is no external source of counterions or salt, the solvent drag on the trapped counterions is transferred to the chains. The idea is that the counterions are slaved to the chains by electrostatic forces, so that the total hydrodynamic drag per blob is effectively the sum of the direct blob contribution and the drag on the counterions associated with the blob. Since the counterions are dilute in the grafted layer and (unlike the monomers) physically unconnected, the counterion contribution may be approximated by the total drag on a collection of *independent* Stokes spheres; *i.e.* hydrodynamic interactions *between* the counterions may be ignored. Since there are of order $\alpha\nu^{-1/3}(\xi/a)^{5/3}$ counterions associated with a blob of size ξ, the counterion contribution to the drag on this blob scales as $[\eta Vb]\times[\alpha\nu^{-1/3}(\xi/a)^{5/3}]$, where b is the effective Stokes radius of the counterion. For simplicity, we assume $b \simeq a$.[34] Then, the total effective drag on a blob $\xi(z)$ at height z scales as

$$f_{\text{h}} = c_1\eta V\xi[1 + c_2\alpha\nu^{-1/3}(\xi/a)^{2/3}] \quad (6)$$

where c_1 and c_2 are unknown numerical constants, which we shall set to unity. For weakly charged chains ($\alpha \ll 1$) in good solvent conditions ($\nu \simeq 1$), the drag is dominated by the polymer contribution. This is true also under Θ solvent conditions where the stretching of chains in the unperturbed brush is determined by ternary repulsive interactions between monomers. For significantly charged chains, the second term of eq 6 becomes significant as the solvent becomes poor for the grafting chains and the brush collapses.[35] However, for the weakly charged limit and the good solvent conditions considered in this paper, the counterion drag contribution is never large.

In mechanical equilibrium, the drag force f_{h} is balanced by the differential tension $\Delta t = (\partial t/\partial z)|_{\text{n}}\xi(z)$ on a blob. Using eqs 5 and 6, this force balance yields the following differential equation for $\xi(z)$:

$$\frac{\mathrm{d}\xi}{\mathrm{d}z}(\xi^{-2} + \xi_0{}^{-2} + \xi^{-1/3}\xi_{\text{e}}{}^{-5/3}) = \xi_{\text{h}}{}^{-2}(1 + (\xi/a)^{2/3}(\xi_{\text{e}}/a)^{-5/3}) \quad (7)$$

where $\xi_{\text{h}} = (kT/\eta V)^{1/2}$ is a characteristic hydrodynamic length, $\xi_{\text{e}} \simeq \alpha^{-3/5}\nu^{1/5}a$ is the characteristic blob size of a charge-dominated brush in the absence of flow, and numerical prefactors of order unity have been suppressed. We may assume that V is approximately uniform throughout the grafted layer.[36] Thus, eq 7 can be formally integrated to give

$$\int_\lambda^{\lambda_0}\mathrm{d}y\frac{y^2 + ry^{5/3} + 1}{y^2 + r(\xi_0/a)^{-1}y^{8/3}} = \frac{\xi_0}{\xi_{\text{h}}{}^2}(H - z) \quad (8)$$

where $\lambda(z) = \xi(z)/\xi_0$ and λ_0 is its value in the limit of zero flow, given by the solution of the equation

$$\lambda_0{}^2 + r\lambda_0{}^{5/3} - 1 = 0 \quad (9)$$

Here the charging parameter $r = (\xi_0/\xi_{\text{e}})^{5/3} \propto \alpha$ has been introduced. The polyelectrolyte effects in the unperturbed brush are strong for $r \gg 1$. Note that $r = n_{\text{ch}}/n_{\text{b}}$, which is the ratio of the number of charges per chain, $n_{\text{ch}} = \alpha N$, to the number of blobs in an unperturbed *neutral* Alexander−de Gennes brush, $n_{\text{b}} = N(\xi_0/a)^{-5/3}\nu^{1/3}$. In the weak charge limit considered in this paper, the denominator of the integrand in eq 8 may be expanded in powers of $\beta = r\lambda^{2/3}a/\xi_0$ and the integral may then be performed analytically. (Note that the expansion parameter satisfies $\beta \ll 1$ for $\alpha \ll 1$). To lowest order in β, the dominant contributions yield an equation of the form

$$\lambda(z)^2 + r\lambda(z)^{5/3} - 1 + 3r\frac{a}{\xi_0}\lambda(z)[\lambda(z)^{-1/3} - \lambda_0{}^{-1/3}] + \lambda(z)\frac{V}{V_0}\frac{(H - z)}{\xi_0} = 0 \quad (10)$$

where $V_0 = kT/(\eta\xi_0{}^2)$.

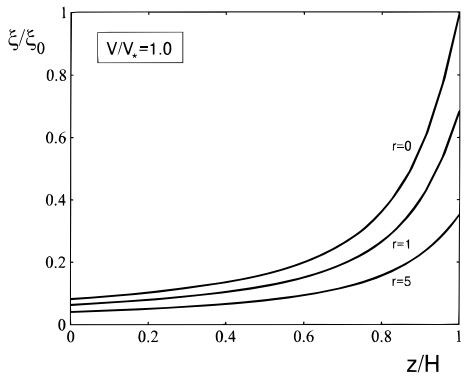

Figure 2. Plots of the reduced local hydrodynamic blob size $\xi(z)/\xi_0$ as a function of the reduced distance z/H from the grafting surface for a reduced permeation flow rate $V/V_* = 1.0$ and for $r = n_{ch}/n_b = 0$ (upper curve), $r = 1.0$ (middle curve), and $r = 5.0$ (lower curve).

For a given brush thickness H, eqs 9 and 10 determine $\xi(z)$ as a function of V and v, and the brush parameters α, N, and ξ_0. However, the brush thickness is constrained by the requirement that a chain of blobs stretched to height H has N monomers via

$$N = c_3 v^{-1/3} \int_0^H \frac{dz}{\xi} \left(\frac{\xi}{a}\right)^{5/3} \tag{11}$$

where c_3 is an unknown numerical constant, which for convenience we will set to unity. The complete solution is obtained by solving eqs 9−11 in a self-consistent manner.

2.3. Results. Figure 2 shows a selection of plots of ξ/ξ_0 vs z/H for several values of $r = n_{ch}/n_b$ and for $V/V_* = 1$, where $V_* = V_0/n_b$ is the characteristic solvent velocity separating the weak and strong deformation regimes for a chain in a *neutral* brush composed of n_b equilibrium blobs[24] and where we have set $n_b = 10$ and $\xi_0/a = 25$. Note that V_* corresponds to a drag force kT/ξ_0 per chain, which coincides with the elastic restoring force per chain in an unperturbed neutral brush. The principal results are that (i) ξ is systematically smaller for the more strongly charged chains (as expected, since in equilibrium charged chains are more stretched than neutral ones at the same solvent quality) and (ii) the variation of $\xi(z)$ with z is much weaker for the more strongly charged chains; *i.e.* the charged chains are more uniformly extended. This is especially true at larger V. It should be mentioned that the continuum treatment for $\xi(z)$ is valid only until the final blob in the extended chain is reached.[37] (Hence, the last blob on a chain occurs somewhat before $z/H = 1$, a feature not correctly represented in Figure 2.)

Perhaps the most important and experimentally accessible property of these deformed brushes is their thickness H as a function of V and α. Figure 3 shows a log−log plot of the reduced brush thickness $h = H/H_0$ as a function of the reduced solvent velocity V/V_* for $r = 0$, 1, and 5, where $H_0 = N\xi_0^{-2/3}v^{1/3}a^{5/3}$ is the scaling result for the height of a *neutral* Alexander−de Gennes brush in the absence of flow. For $r \ll 1$, we recover the results of ref 24 for neutral brushes: For $V \ll V_*$, $H \sim N$, while for $V \gg V_*$, $H \sim N^3 V^2$, as for isolated tethered chains in flows.[28] As r increases, the crossover region between these two limits shifts to slightly higher V and becomes somewhat broader. In principle, all curves eventually fall on the same master curve for sufficiently large V. However, these results for $H(V)$ are limited by finite extensibility effects; for sufficiently large V,

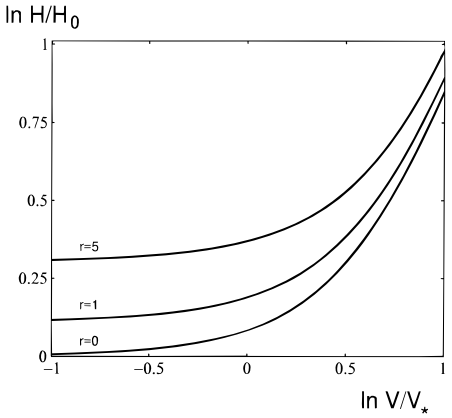

Figure 3. Double-logarithmic plot of the reduced brush thickness H/H_0 as a function of the reduced solvent permeation flow rate V/V_* for $r = 0$ (lower curve), $r = 1$ (middle curve), and $r = 5$ (upper curve), where $V_* = kT/(\eta\xi_0^2 n_b)$ and $H_0 = N\xi^{-2/3}v^{1/3}a^{5/3}$.

chains are fully extended ($H \simeq Na$) and this analysis breaks down. For the case presented in Figure 3 ($n_b = 10$ and $\xi_0/a = 25$), full extension ocurrs for $V/V_* \gtrsim 10$.

2.4. Monoblock Approach. For neutral brushes in flow, the analysis of ref 24 showed that a simplified "monoblock" picture[28] gave essentially equivalent asymptotic results for $H(V)$ as in a more detailed local analysis, like that described above. The monoblock approach has the advantage of a more intuitive presentation of the underlying physics, so we briefly discuss it here. In this approach, one views a chain as a *uniformly* extended string of hydrodynamic Pincus blobs of *effective* blob size $\xi_{mb} \le \xi_0$ with total length $H \sim N\xi_{mb}^{-2/3}a^{5/3}v^{1/3}$. The brush thickness H is then obtained by balancing the global chain tension $\partial F/\partial H$ with the total hydrodynamic drag on the chain. Consider first the limit of local electroneutrality, $\lambda_D \ll H$. In this case, the total free energy per chain, $F = F_{el} + F_{int} + F_{ion}$ from eqs 1−3, may be written explicitly in terms of H within the monoblock picture as

$$\frac{F}{k_B T} \simeq \left(\frac{H}{R_F}\right)^{5/2} + \frac{R_F^{5/2}}{\xi_0^2 H^{1/2}} + \alpha N \log\left(\frac{\alpha N a^3}{\xi_0^2 H}\right) \tag{12}$$

where $R_F = N^{3/5}a$ is the Flory radius of an isolated chain. The total hydrodynamic drag on a chain in the monoblock picture is roughly the product of the drag on a blob of size ξ_{mb}, given by eq 6 with $\xi = \xi_{mb}$, and the total number H/ξ_{mb} of such blobs per chain:

$$f_{tot} \simeq \eta V(H + \alpha N a) \tag{13}$$

Balancing the total drag on a chain with the global chain tension $\partial F/\partial H$ gives

$$h^3 - n_b \frac{V}{V_0} h^{5/2} - n_{ch} \frac{a}{\xi_0} \frac{V}{V_0} h^{3/2} - \frac{n_{ch}}{n_b} h^{1/2} - 1 = 0 \tag{14}$$

where $h = H/H_0$ and $V_0 = kT/(\eta\xi_0^2)$. The first term proportional to V/V_0 in eq 14 is from the polymer contribution to chain drag, while the second is due to the counterions.

For weak flows, h is determined by the first term and the last two terms of eq 14 (cf. eq 9), while for strong flows, the first three terms determine h. The monoblock results for H/H_0 as a function of V/V_* and $r = n_{ch}/n_b$ are in qualitative agreement with the more detailed local

analysis presented above. One can identify two characteristic solvent velocities from eq 14: V_* separating the weak and strong deformation regimes in the absence of charge, and $V_{**} \simeq kT/(\eta\xi_e^2 n_{ch}) = r^{1/5}V_*$ separating these regimes for charge-dominated brushes. Note that for reasonable values of r, V_* and V_{**} are not very different. For $r \ll 1$, we recover the results of ref 24 for neutral brushes: For $V \ll V_*$, $H \sim$ N, while for $V \gg V_*$, $H \sim N^3V^2$.[38] As r increases, the crossover region between these two limits shifts to slightly higher V and becomes somewhat broader. In this regime, both V_* and V_{**} are playing a role. This explains the shift and the apparent broadening of the crossover region with increasing r found in the local analysis. For realistic values of r, the counterion drag mechanism never dominates; rather it slightly modifies the behavior of the crossover region. For charge-dominated brushes in equilibrium, there is roughly one charge per blob,[5] and hence there is on average one counterion associated with each blob. For situations modelled here, the equilibrium blob size is much larger than the effective hydrodynamic radius of a counterion,[39] so the hydrodynamic drag is dominated by the polymer contribution. As the chain is extended in flow, the blob size becomes smaller than its equilibrium value, but the counterion density also decreases, maintaining the dominance of the polymer drag term.

Up to now we have only considered the behavior of polyelectrolyte brushes under the conditions when local electroneutrality is satisfied. In this limit, the brush is in the so-called "osmotic" regime, in which the osmotic pressure of counterions is the dominant polyelectrolyte effect. However, for $\alpha \gg N^{-1}(\xi_0/l_B)^{1/2}$ there is a range of grafting densities for which electrostatic interactions in the brush play a dominant role but the local electroneutrality condition is violated.[5,9] In this regime, the surface charge density due to the grafted polyions is not large enough to retain all the mobile counterions inside the brush. As a result the counterions are free to explore a layer of thickness $\lambda_D \cong \xi_0^2/(l_B\alpha N)$ above the grafting surface. We remark that the thickness of the counterion cloud in this case is much greater than the brush thickness, so that almost all the counterions leave the brush. In the framework of a monoblock picture we can utilize a simplified "capacitor" model in which the grafted polyions and the counterion cloud form two oppositely charged layers (each with charge per unit area of magnitude $\alpha N/\xi_0^2$). This results in a Coulomb force per chain of order $l_B(\alpha N)^2/\xi_0^2$ which stretches the chain perpendicular to the grafting surface. Hence in the absence of the flow, each chain can be represented[9] as a chain of electrostatic blobs of size $\xi_q \cong \xi_0^2/(l_B\alpha^2N^2)$. Let us mention that a more rigorous analysis[40] indicates that the fluctuations of the position of the free chain ends in this regime are less important than in osmotic brushes. Thus the Alexander−de Gennes approximation and the monoblock picture used here are likely to be qualitatively adequate.

In order to obtain the equation for the thickness of the brush in a normal permeation flow, we must balance the modified global chain tension

$$\frac{\partial F}{\partial H} \simeq kT\left(\frac{H^{3/2}}{R_F^{5/2}} - \frac{R_F^{5/2}}{\xi_0^2 H^{3/2}} - l_B\frac{(\alpha N)^2}{\xi_0^2}\right) \qquad (15)$$

with the hydrodynamic drag per chain, $f_h \cong \eta V(H + \alpha Na)$. Note that, as before, the counterion contribution to the hydrodynamic drag is small. The final equation for the reduced brush thickness h in the "capacitor" regime reads

$$h^3 - n_b\frac{V}{V_0}h^{5/2} - n_{ch}^2\frac{l_B}{\xi_0}h^{3/2} - 1 = 0 \qquad (16)$$

where we have suppressed the small counterion drag contribution. As before, one can identify two characteristic solvent velocities from eq 16: V_* separating the weak and strong deformation regimes in the absence of charge, and a modified $V_{**} \simeq V_*(l_B/\xi_0)^{1/3}n_{ch}^{2/3}$ separating these regimes for charge-dominated brushes. Note that V_{**} in the "capacitor" regime grows more rapidly with n_{ch} than in the "electroneutrality" regime. Once again, however, for $V \gg V_*$ and $V \gg V_{**}$, the $H \sim N^3V^2$ behavior dominated by the hydrodynamic drag due to flow is recovered.

3. Shear Flows

We now consider the case of shear flows, in which the brush is subjected to a flow $\mathbf{V} = \dot{\gamma}z\hat{x}$ parallel to the grafting surface. In the presence of strong shear flow, the grafted chains stretch and tilt away from the normal direction, leading to a somewhat distorted brush within which there is some solvent flow profile $\mathbf{V} = V(z)\hat{x}$. We picture this deformed brush as consisting of tilted chains of Pincus blobs,[27] as sketched in Figure 4. Since the chain extension is due to the integrated hydrodynamic drag on each chain rather than a force applied to the chain ends, the hydrodynamic Pincus blob size ξ and chain tilt angle θ are not constants, but are functions of the distance from the grafting plane which we must determine self-consistently with the solvent flow profile in the brush.

3.1. Free Energy and Effective Tension. In the case of shear flows, we will restrict our attention to locally electroneutral brushes in the limit $\alpha \ll (l_B/a)^{-2}$, for which the free energy per chain is the sum of three terms: an elastic term F_{el} involving chain deformation, an osmotic term F_{int} involving interactions between blobs, and a mixing term F_{ion} accounting for the entropy of mixing of the mobile counterions. For nonuniformly stretched and tilted polyelectroltye chains, these take the form

$$\frac{F_{el}}{k_BT} \simeq \int_0^L \frac{ds}{\xi(s)} \qquad (17)$$

$$\frac{F_{int}}{k_BT} \simeq \xi_0^{-2}\int_0^L ds\frac{\xi(s)}{\cos\theta(s)} \qquad (18)$$

$$\frac{F_{ion}}{k_BT} \simeq \alpha v^{-1/3}a^{-5/3}\int_0^L ds\xi(s)^{2/3}\log\left[\frac{\alpha\xi(s)^{2/3}a^{4/3}}{v^{1/3}\xi_0^2\cos\theta(s)}\right] \qquad (19)$$

where s is an arc length coordinate, $\theta(s)$ is the local tilt angle measured from the $\hat{z}$ direction, and L is the total arc length of a tilted string of blobs. Equations 17 and 18 are identical to those previously used to model the of behavior of neutral grafted polymers in good solvent shear flows.[25] The factors of cos θ in eqs 18 and 19 account for the corrections to the polymer blob and counterion volume fractions due to the tilting of the chains in shear flows.

Using eqs 17−19 and the procedure developed in ref 25, one can define an effective chain tension $\mathbf{t}(s)$ as follows. Consider a short section of chain of length Δs containing Δn monomers. Equations 17−19 give the

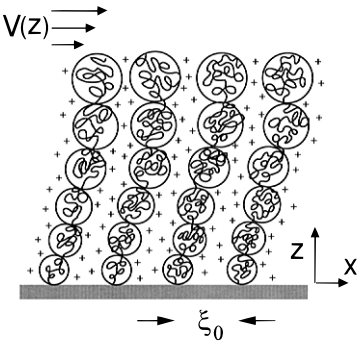

Figure 4. Sketch of a deformed polyelectrolyte brush in a strong solvent shear flow $\mathbf{V}(z) = \dot{\gamma} z \hat{x}$ parallel to the grafting surface.

free energy of this section of chain as

$$\Delta F \simeq kT\left(\frac{1}{\xi(s)} + \frac{\xi(s)}{\xi_0^{\,2}\cos\theta(s)} + \frac{\alpha\xi(s)^{2/3}}{v^{1/3}a^{5/3}}\log\left[\frac{\alpha\xi(s)^{2/3}a^{4/3}}{v^{1/3}\xi_0^{\,2}\cos\theta(s)}\right]\right)\Delta s \quad (20)$$

where we have omitted all unknown numerical prefactors. This expression may be written exclusively in terms of Δx, Δz, and Δn by using $\Delta s^2 = \Delta x^2 + \Delta z^2$, $\cos\theta = \Delta z/\Delta s$, and the local chain stretching expression for Pincus blobs,[27] $\Delta s \simeq \xi^{-2/3}a^{5/3}\Delta n$, to eliminate ξ and θ from ΔF. Subsequent variation of ΔF with respect to Δx at fixed Δn and Δz, and of ΔF with respect to Δz at fixed Δn and Δx give the components t_x and t_z of the effective local chain tension as

$$\frac{t_x(s)}{k_BT} = t_1\frac{\sin\theta(s)}{\xi(s)} + t_2\frac{\xi(s)}{\xi_0^{\,2}}\tan\theta(s) \quad (21)$$

$$\frac{t_z(s)}{k_BT} = t_1\frac{\cos\theta(s)}{\xi(s)} - t_2\frac{\xi(s)}{\xi_0^{\,2}}\left(\frac{2-\cos^2\theta(s)}{\cos^2\theta(s)}\right) - t_3\frac{\alpha\xi(s)^{2/3}}{v^{1/3}a^{5/3}\cos\theta(s)} \quad (22)$$

where t_1, t_2, and t_3 are positive constants of order unity. Once again, this effective tension determines the local departure from equilibrium of a representative chain, under conditions where all chains are constrained to behave identically, and hence already contains all osmotic terms. As before, the unknown constants in eqs 21 and 22 may be fixed by insisting on equilibrium chain behavior in the limit of $t = 0$; this requirement is satisfied if we set $t_1 = t_2 = t_3 = 1$.

3.2. Hydrodynamic Forces. In mechanical equilibrium, the total hydrodynamic drag on a blob $\xi(s)$ at $z(s)$ must be balanced by the differential tension across the blob. Assuming laminar flow with $\mathbf{V}||\hat{x}$ in the brush, the total hydrodynamic drag on a blob is also in the $\hat{x}$ direction. For the case of shear flows, there are nontrivial electrokinetic effects to consider. Unlike the case of normal permeation flows, the counterions are somewhat free to move with the solvent. However, there are some restrictions on counterion convection: in actual flow conditions, ions are subject to the effects of electric fields produced by their local rearrangement in flow and to the particular boundary conditions on ion current or electric potential. A complete analysis of such electrokinetic effects is beyond the scope of this work. However, in realistic situations one expects electrokinetic effects that are intermediate to the cases of "bound" counterions considered in the previous section and unrestricted counterion flow that would occur for a perfect current source. In the following, we will focus on the idealized case of freely convecting counterions. In this case there is no counterion contribution to polyelectrolyte drag in flow[41] and the total hydrodynamic drag on a blob is $\mathbf{f}_h \simeq \eta\xi(s)V(s)\hat{x}$, the bare polymer contribution. Mechanical force balance then implies $t_z = 0$ and $\Delta t_x = (\partial t_x(s)/\partial s)\xi(s) = c_1\eta V(s)\Delta s$, where c_1 is a dimensionless constant discussed below. These requirements lead to

$$\frac{t_x(z)}{k_BT} = \frac{\sin\theta(z)}{\xi(z)} + \frac{\xi(z)}{\xi_0^{\,2}}\tan\theta(z) = c_1\frac{\eta}{k_BT}\int_z^H dz'\frac{V(z')}{\cos\theta(z')} \quad (23)$$

$$\cos^3\theta(z) - \left(\frac{\xi(z)}{\xi_0}\right)^2(2-\cos^2\theta(z)) - r\left(\frac{\xi(z)}{\xi_0}\right)^{5/3}\cos\theta(z) = 0 \quad (24)$$

where H is the thickness of the deformed brush and where we have changed the independent variable to z, the normal distance from the grafting surface. Equation 24 enforces $t_z = 0$ in the brush.

The shear stress σ_{xz} in the brush is the sum of the contributions from the viscous dissipation due to solvent flow, $\sigma_{xz}^{(s)} = \eta\, dV/dz$, and from the elastic deformation of polymer chains, $\sigma_{xz}^{(p)}$. The polymer contribution $\sigma_{xz}^{(p)}$ is approximately given by the product of the effective lateral chain tension $t_x(z)$ and the number density of chains crossing the plane at height z : $\sigma_{xz}^{(p)} \simeq t_x(z)/\xi_0^2$. Requiring that, in the absence of inertial effects, the total shear stress is uniform throughout the grafted layer gives an additional relation between the chain conformations and the solvent velocity in the brush,

$$\frac{d^2V}{dz^2} = c_2\frac{1}{\xi_0^{\,2}}\frac{V(z)}{\cos\theta(z)} \quad (25)$$

where c_2 is another dimensionless constant of order unity. Equations 23−25 are subject to appropriate boundary conditions at $z = 0$ and $z = H$. We assume no-slip boundary conditions at the grafting surface and continuity of shear stress at the free surface of the brush. Furthermore, we assume that the effective tension, eq 23, vanishes at the free end of each chain. Thus, our boundary conditions are $V = 0$ at $z = 0$, and $dV/dz = \dot{\gamma}$ and $\theta = 0$ at $z = H$. Furthermore, $\theta(H) = 0$ implies $\xi(H)$ must take its equilibrium value, given by the solution of eq 24 with $\theta = 0$.[37]

For a given brush thickness H, eqs 23−25 together with the above boundary conditions uniquely determine $V(z)$, $\xi(z)$, and $\theta(z)$ as functions of the solvent shear rate outside the brush $\dot{\gamma}$, and the equilibrium brush parameters N, α, and ξ_0. The appropriate brush thickness is then obtained by demanding that a chain of blobs stretched to height H has N monomers via the conser-

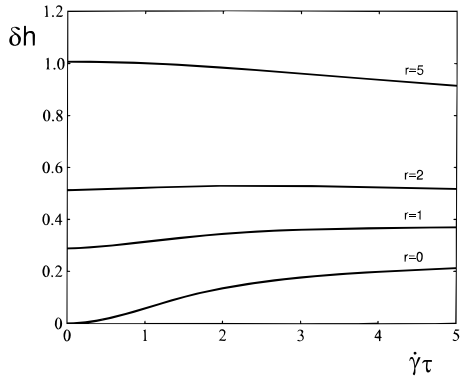

Figure 5. Plots of the relative brush swelling $\delta h = (H - H_0)/H_0$ vs $\dot{\gamma}\tau$ for brushes with $r = 0$ (lower curve), $r = 1$, $r = 2$, and $r = 5$ (upper curve).

vation relation

$$N = c_3 v^{-1/3} \int_0^H \frac{\mathrm{d}z}{\xi(z) \cos \theta(z)} \left(\frac{\xi(z)}{a}\right)^{5/3} \tag{26}$$

where c_3 is another constant of order unity.

The solution of eqs 23−26 requires a numerical approach. To facilitate this analysis, we choose for definiteness to set the unknown numerical constants c_1, c_2, and c_3 to unity. It is also convenient to recast eq 23 into a differential form

$$\frac{\mathrm{d}\xi}{\mathrm{d}z} = \frac{V\xi^2 \cos \theta / V_0}{[\sin \theta \cos \theta(\xi^2 - {\xi_0}^2 \cos \theta) + \xi\theta'(\xi^2 + {\xi_0}^2 \cos^3 \theta)]} \tag{27}$$

where $V_0 = kT/(\eta\xi_0^2)$, $\theta' = d\theta/d\xi$.

3.3. Results. We have studied the solution of eqs 24−27 plus boundary conditions as a function of the dimensionless shear rate $\dot{\gamma}\tau$, where $\tau = \eta\xi_0^3/k_BT$ is of order the characteristic relaxation time of a Zimm blob of radius ξ_0, and as a function of the equilibrium brush parameters N, α, and ξ_0. Figure 5 shows plots of the relative brush swelling $\delta h = (H - H_0)/H_0$ vs $\dot{\gamma}\tau$ for brushes with $r = 0$, 1, 2, and 5 and for fixed N and ξ_0, where $H_0 = N\xi_0^{-2/3}v^{1/3}a^{5/3}$ is the equilibrium thickness of the equivalent neutral Alexander−de Gennes brush. For a neutral brush ($r = 0$), the onset of significant brush swelling occurs at $\dot{\gamma}\tau \simeq 1$, followed by a saturation of swelling at large $\dot{\gamma}\tau$ of $\delta h \simeq 0.25$. With increasing r, brush swelling effects are progressively suppressed. At $r = 2$, δh is essentially independent of shear rate, having only a very weak maximum near $\dot{\gamma}\tau = 2.5$. For $r \gtrsim 2$, the brush thickness is actually a decreasing function of shear rate. This reversal in the response of $\delta h(\dot{\gamma})$ with increasing r is in qualitative accord with the predictions of ref 22 for the response of polyelectrolyte brushes to imposed shear boundary forces.

For weakly charged (quasi-neutral) brushes, $r \ll 1$, the dominant osmotic contribution to the free energy per chain comes from the interaction between polymer blobs. In good solvent conditions, this interaction couples the normal and tangential response of a brush to solvent flow, leading to swelling in the normal direction in response to external forces in the tangential direction. The origin of this swelling is an increase in the osmotic pressure in the brush due to the reduction of screening of excluded volume interactions in response to lateral extention of the chains in shear flow.

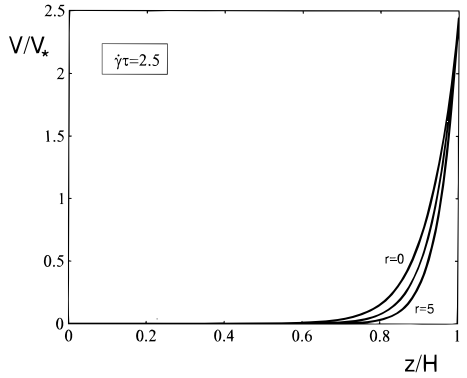

Figure 6. Plots of the reduced solvent velocity profiles V/V_0 as a function of the reduced distance z/H from the grafting surface for brushes with $r = 5$ (lower curve), $r = 2$ (middle curve), and $r = 0$ (upper curve), all sheared at $\dot{\gamma}\tau = 2.5$. Although the brush heights H are increasing functions of r, the hydrodynamic penetration length is found to be $l_p \simeq \xi_0$, independent of r.

In the charge-dominated regime, $r \gtrsim 1$, the dominant osmotic contribution to the free energy comes from the mobile counterion entropy of mixing. Since this contribution only affects chain extension normal to the grafting surface (*cf.* eqs 21 and 22), there is no coupling of the normal and tangential response of a brush to solvent flow due to the counterions: the osmotic pressure of counterions inside the brush does not depend on the degree of chain extension in the lateral direction. This leads to gradual decrease in the brush thickness under shear flows in the charge-dominated regime. An osmotic pressure of counterions of order $\sim kT\alpha^{1/2}$ per chain opposes this decrease more efficiently as the fraction of charged monomers α increases. Furthermore, since in the absence of flow the chains in charged brushes are already relatively extended compared with chains in an equivalent neutral brush, relatively higher shear rates are required to produce the same magnitude of deformation $|\delta h|$ in the charged-dominated regime; charged brushes are less susceptible to deformation in flow than neutral ones.

This latter point can be clarified by examining the internal brush structure and solvent velocity profiles for several different charged brushes subjected to the same solvent shear rate. Figure 6 shows the scaled internal solvent velocity profiles V/V_0 *vs* z/H for brushes with $r = 0$ (upper curve), $r = 2$ (middle curve), and $r = 5$ (lower curve) subjected to an external solvent shear rate $\dot{\gamma}\tau = 2.5$. Although the brush height H depends strongly on r (reflected by the differences between the curves in Figure 6), the hydrodynamic penetration depth calculated from the velocity profiles, $l_p \equiv [V(H)/V'(H)] \simeq \xi_0$, is roughly independent of r. Figure 7 shows profiles of the associated tilt angle θ and the scaled blob size ξ/ξ_0. The upper, middle, and lower curves in the figure and inset correspond to $r = 0$, 2, and 5, respectively. (Note that, as in the case of permeation flows, the last blob on a chain actually occurs somewhat before $z/H = 1$,[37] a feature not correctly represented in Figures 6 and 7.) Figure 7 shows that the most strongly charged chains ($r = 5$) are at the same time the most uniformly stretched and the least tilted. They are also the least extended relative to their state in the absence of flow. This is consistent with the expectation that brushes of neutral chains are more susceptible to deformation by shear flow than charged ones.

These figures show that, roughly speaking, stretched chains can be divided into two regions: (i) an interior

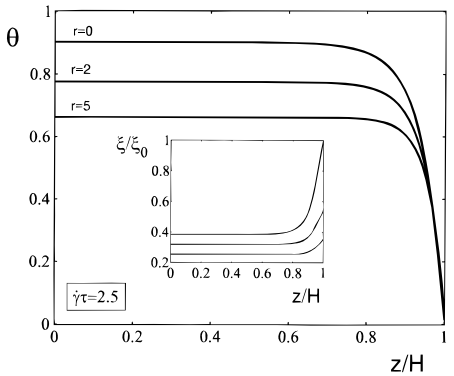

Figure 7. Plots of the tilt angle θ and reduced blob size ξ/ξ_0 vs z/H for $\dot{\gamma}\tau = 2.5$. The main plot shows θ for brushes with $r = 5$ (lower curve), $r = 2$ (middle curve), and $r = 0$ (upper curve), while the inset shows the analogous curves of ξ/ξ_0 vs z/H in the same order.

region of essentially uniform stretching and tilt in which V is very small and (ii) a boundary region of thickness $\Delta z \simeq \xi_0$, corresponding to a hydrodynamic penetration depth l_p which is independent of r, of weakly stretched and tilted chains in which $\xi(z)$ and $\theta(z)$ vary rapidly. Furthermore, the net variation of θ and ξ between the interior region and the free surface is systematically smaller for larger r; the more strongly charged the chains, the more uniform their deformation. From the point of view of hydrodynamic drag, these results can be viewed in terms of a "quasi-monoblock" picture[25] in which uniformly tilted and stretched chains with constant blob size ξ_{mb} and tilt angle θ_{mb} terminate in an unperturbed *virtual* end-blob of size $\xi_{end} \simeq \xi_0$ (which is independent of charge fraction). In such a picture, the brush behavior in flow may be understood in terms of the response of the uniformly deformed portion of the grafted chains to a shear force $f_{||} \sim \eta\dot{\gamma}\xi_0^2$ due to the hydrodynamic drag on this *virtual* end-blob. Such a "quasi-monoblock" picture bridges the present calculation with the approaches of refs 19, 20, and 22. We note that the extension of this analysis to shear flows in the "capacitor regime", $\lambda_D \gg H$, described in section 2.4 is rather subtle, since the behavior of the counterion cloud is probably rather sensitive to the details of the electrokinetic effects mentioned above. However, we expect that counterion osmotic effects will be somewhat weaker in this limit relative to brushes in the "electroneutral" limit analyzed above.

4. Discussion

We have presented a coherent theoretical approach for modeling the behavior of grafted polyelectrolyte layers in strong normal and shear flows of good solvent. This approach allows one to account for the nonuniform deformation of grafted polyelectrolyte chains in strong solvent flows. Furthermore, in the case of shear flows, the solvent flow profile within the layer and the deformation of the layer are obtained in a mutually consistent fashion (for permeation flows, the solvent flow rate is externally controlled by an applied pressure difference across the brush[24]). This model represents the extension to polyelectrolyte brushes of previous models for the deformation of neutral Alexander−de Gennes type brushes in strong flows.[24,25] One advantage of our approach to brush deformation is that, by explicitly accounting for the solvent hydrodynamics, we are able to make a relatively direct connection to experiments, in which the rate of solvent flow is the appropriate control parameter. Other approaches to neutral[19−21] and polyelectrolyte[22] brush deformation effectively ignore the details of solvent flow inside a brush by modeling the solvent−brush frictional forces by *ad hoc* forces applied to the free surface of a brush, which makes quantitative comparison with experiment difficult.

In general, we find that with increasing charge fraction, polyelectrolyte brushes become less susceptible to deformation in solvent flows. For the case of brushes in solvent flows normal to the grafting surface, strongly charged brushes are more uniformly extended than weakly charged ones (*cf.* Figure 2). Furthermore, the crossover region separating the weak deformation ($H \sim N\xi_0^{-2/3}$) and strong deformation ($H \sim N^3V^2$) regimes shifts to higher solvent flow rates V and becomes somewhat broader with increasing charge fraction (*cf.* Figure 3). A rough estimate of the characteristic flow rate separating the weak and strong deformation regimes is obtained by equating the equilibrium blob size ξ_e in the brush with the hydrodynamic length $\xi_h = (kT/\eta V)^{1/2}$. Since ξ_e is a decreasing function of the charge fraction α, this implies that this characteristic flow rate is an increasing function of the charge fraction. For the case of brushes in shear flows, this reduced susceptibility to flow results in chains that are more uniformly stretched, less extended relative to quiescent conditions, and less tilted with increasing charge fraction, even though the hydrodynamic penetration length of solvent flow into the brush is essentially independent of the charge fraction. Furthermore, the coupling between deformation in the normal and tangential directions becomes progressively weaker with increasing charge fraction, due to the emerging dominance of the counterion osmotic pressure. This effect leads to the reversal of the dependence of brush thickness on shear rate with increasing charge fraction; weakly charged brushes expand in strong shear flows, while more strongly charged brushes collapse somewhat in the same flows (*cf.* Figure 5). This latter phenomenon is in quailitative agreement with the results of ref 22 based on a model of polyelectrolyte brush deformation in response to applied boundary shear forces.

The approach we have described has several inherent limitations. We have adopted a scaling approach based on the Alexander−de Gennes ansatz that all chains stretch alike. (Note however that we did not assume a uniform blob size: this follows from the Alexander−de Gennes ansatz only when flow is absent.) All numerical prefactors are unknown. Furthermore, this approximation systematically underestimates the susceptability of the periphery of the brush to flow and, in the case of shear flows, the hydrodynamic penetration depth of solvent flows into the brush.[18] Thus, the characteristic flow rates marking the onset of brush deformation are expected also to be systematically underestimated. Recent modeling of neutral brush deformation in shear flows that allows for a partial relaxation of the Alexander−de Gennes ansatz appears to support this expectation.[26] However, for the purpose of investigating the charge dependence of brush deformation in solvent flows, the present analysis is expected to reveal the correct trends. Furthermore, a fully self-consistent treatment would require a more detailed analysis of hydrodynamic interactions and electrokinetic effects and would be a formidable numerical task. In the case of shear flows, our results are based on the assumption of freely mobile charge currents transverse to the layer.

Thus, we have not properly accounted for electrokinetic effects. For the case of good solvent conditions and locally electroneutral brushes, we expect only minor quantitative changes due to this assumption. However, there may be interesting modifications arising from changes to the ion drag term in other cases. Finally, our approach is also limited by finite extensibility of the grafted polymer chains. For sufficiently high flow rates, the chains approach full extension and the blob concept employed in our model to estimate elastic and hydrodynamic forces breaks down. This regime, although experimentally relevant, would require a either a substantially modified theoretical analysis or a wholly computational approach.

The approach we have introduced in this paper may be modified to address more general problems involving charged polymer layers in strong flows. The cases of grafted polyelectrolytes in the presence of added salt and of grafted polyampholytes, chains containing both positive and negative charge groups, would be interesting extensions of the present calculation. The dependence of flow-induced polyelectrolyte brush deformation on solvent quality[35] is also an important issue, since polyelectrolyte backbones are marginally soluble in most cases of practical importance. Finally, the issue of flow-induced lateral structural heterogeneities in grafted polymer layers is a very important problem, although the modeling of this behavior may require quite a different approach than we have employed here.

Acknowledgment. The work of J.L.H. and M.E.C. was supported in part by the EPSRC and the DTI Colloid Technology Programme. O.V.B. acknowledges the hospitality of Prof. K. Kramer at the Max-Planck-Institut für Polymerforschung.

References and Notes

(1) Milner, S. T. *Science* **1991**, *251*, 905.
(2) Halperin, A.; Tirrell, M.; Lodge, T. P. *Adv. Polym. Sci.* **1992**, *100*, 33.
(3) Miklavic, S. J.; Marcelja, S. *J. Phys. Chem.* **1988**, *92*, 6718.
(4) Misra, S.; Varanasi, S.; Varanasi, P. P. *Macromolecules* **1989**, *22*, 4173.
(5) Pincus, P. *Macromolecules* **1991**, *24*, 2912.
(6) Borisov, O. V.; Birshtein, T. M.; Zhulina, E. B *J. Phys. II Fr.* **1991**, *1*, 521.
(7) Zhulina, E. B.; Borisov, O. V.; Birshtein, T. M. *J. Phys. II Fr.* **1992**, *2*, 63.
(8) Ross, R. S.; Pincus, P. *Macromolecules* **1992**, *25*, 2177.
(9) Borisov, O. V.; Zhulina, E. B.; Birshtein, T. M. *Macromolecules* **1994**, *27*, 4795.
(10) Misra, S.; Mattice, W. L.; Napper, D. H. *Macromolecules* **1994**, *27*, 7090.
(11) Zhulina, E. B.; Birshtein, T. M.; Borisov, O. V. *Macromolecules* **1995**, *28*, 1491.
(12) Zhulina, E. B.; Borisov, O. V. *Macromolecules* **1996**, *29*, 2618.
(13) Klein, J.; Perahia, D.; Warburg, S. *Nature* **1991**, *352*, 143.
(14) Klein, J. *Colloids Surf. A* **1994**, *86*, 63.
(15) Klein, J.; Kumacheva, E.; Perahia, D.; Mahalu, D.; Warburg, S. *Faraday Discuss.* **1994**, *98*, 173.
(16) Klein, J. *Annu. Rev. Mater. Sci.* **1996**, *26*, 581.
(17) Fredrickson, G. H.; Pincus, P. *Langmuir* **1991**, *7*, 786.
(18) Milner, S. T. *Macromolecules* **1991**, *24*, 3704.
(19) Rabin, Y.; Alexander, S. *Europhys. Lett.* **1990**, *13*, 49.
(20) Barrat, J.-L. *Macromolecules* **1992**, *25*, 832.
(21) Kumaran, V. *Macromolecules* **1993**, *26*, 2464.
(22) Birshtein, T. M.; Zhulina, E. B. *Makromol. Chem., Theory Simul.* **1992**, *1*, 193.
(23) Williams, D. R. M *Macromolecules* **1993**, *26*, 5808.
(24) Harden, J. L.; Cates, M. E. *J. Phys. II Fr.* **1995**, *5*, 1093, 1757 (erratum).
(25) Harden, J. L.; Cates, M. E. *Phys. Rev. E* **1996**, *53*, 3782.
(26) Aubouy, M.; Harden, J. L.; Cates, M. E. *J. Phys. II Fr.* **1996**, *6*, 969.
(27) Pincus, P. *Macromolecules* **1976**, *9*, 386.
(28) Brochard-Wyart, F. *Europhys. Lett.* **1993**, *23*, 105. Brochard-Wyart, F.; Hervet, H.; Pincus, P. *Europhys. Lett.* **1994**, *26*, 511.
(29) Alexander, S. *J. Phys. Paris* **1977**, *38*, 983.
(30) De Gennes, P. G. *J. Phys. Paris* **1976**, *37*, 1443; *Macromolecules* **1980**, *13*, 1069.
(31) Milner, S. T.; Witten, T. A.; Cates, M. E. *Europhys. Lett.* **1988**, *5*, 413; *Macromolecules* **1988**, *21*, 2610.
(32) Skvortsov, A. M.; Gorbunov, A. A.; Pavlushkov, I. V.; Zhulina, E. B.; Borisov, O. V.; Priamitsyn, V. A. *Polym. Sci. USSR (Engl. Transl.)* **1988**, *30*, 1706. Zhulina, E. B.; Borisov, O. V.; Pryamitsyn, V. A. *J. Colloid Interface Sci.* **1990**, *137*, 495.
(33) F_{ion} can be important for grafted polyampholytes, however. See also ref 6 for discussion.
(34) The effective Stokes radius of a counterion is the sum of the bare ion size and the thickness of the hydration shell around it. The bare ion size may be much smaller than a, but the thickness of the hydration shell can be substantial.
(35) Harden, J. L., submitted to *Macromolecules*.
(36) Spatial corrections to $V(z)$ due to polymer density variations in the $\hat{z}$ direction are small for the semidilute conditions in a good solvent brush. So, although they may in principle be considered, they do not qualitatively change the results presented here.
(37) The final blob in an extended chain occurs at $z \simeq H - \xi_{max}$, where ξ_{max} is the size of this last blob. This technical detail does not qualitatively affect any of our conclusions.
(38) In the monoblock picture, however, the crossover region is sharper than in the local analysis.
(39) Otherwise, the blob concept breaks down entirely and α is so large that the presence of charge modifies the chain statistics.
(40) Borisov, O. V.; Zhulina, E. B., submitted to *J. Phys. Fr. II*.
(41) We expect that since the counterion contribution to the polyelectrolyte drag is in general small for good solvent conditions, our results will not be significantly affected by this approximation.

MA9612337